Thickness Controlled Water Vapors Assisted Growth of Multilayer Graphene by Ambient Pressure Chemical Vapor Deposition

ARTICLE *in* THE JOURNAL OF PHYSICAL CHEMISTRY C · JANUARY 2015

Impact Factor: 4.77 · DOI: 10.1021/jp510106w

6 AUTHORS, INCLUDING:

Muhammad Asif
Dalian University of Technology
27 PUBLICATIONS **164** CITATIONS
SEE PROFILE

Lujun Pan
Dalian University of Technology
90 PUBLICATIONS **1,182** CITATIONS
SEE PROFILE

Muhammad Usman
Dalian University of Technology
4 PUBLICATIONS **8** CITATIONS
SEE PROFILE

THE JOURNAL OF PHYSICAL CHEMISTRY C

Article

pubs.acs.org/JPCC

Thickness Controlled Water Vapors Assisted Growth of Multilayer Graphene by Ambient Pressure Chemical Vapor Deposition

Muhammad Asif,*[,†,‡] Yi Tan,[†] Lujun Pan,*[,‡] Jiayan Li,[†] Muhammad Rashad,[§] and Muhammad Usman[‡]

[†]School of Materials Science and Engineering, Dalian University of Technology, Dalian 116024, People's Republic of China

[‡]School of Physics and Optoelectronics, Dalian University of Technology, Dalian 116024, People's Republic of China

[§]College of Materials Science and Engineering, Chongqing University, Chongqing 400044, People's Republic of China

Supporting Information

ABSTRACT: Chemical vapor deposition graphene growth results are inconsistent, specifying that crucial growth parameters still remain unknown or uncontrolled. In the current study, we demonstrate that water can be used as a special tool to control thickness and size of graphene islands, during ambient pressure chemical vapor deposition growth of graphene. Large area bilayer graphene was synthesized using optimized conditions in the absence of water, which was later used as a reference condition for water assisted growth of multilayer graphene (MLG), by introducing water vapors during the growth stage. Raman spectroscopy, UV−vis spectroscopy, and transmission electron microscopy were used to estimate the quality and thickness of graphene. It was observed that graphene thickness increases from 2 to 25 layers with increase in water vapors ranging from 0 to 2000 ppmv, which revealed significant improvement in growth rate. Scanning electron microscopy results exhibited growth of discontinuous graphene islands which reveal the etching behavior of water vapors. In conclusion, water plays a dual role during growth of graphene, i.e. speeding up growth rate, subsequently resulting in MLG growth, as well as etching of graphene edges.

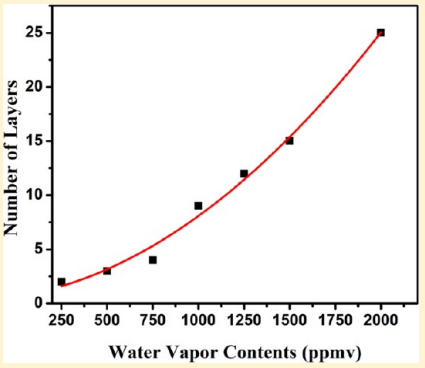

1. INTRODUCTION

Graphene, a single atom thick sheet of sp^2-hybridized carbon atoms arranged in a hexagonal honeycomb lattice crystal structure, has attracted great interest among numerous fields of research. Due to unique electronic,[1] optical,[2] mechanical,[3] thermal,[4] and electrochemical[5] properties, graphene has become a potential future material for numerous applications ranging from electronics and photonics, to energy storage and solar cells.[6−12] To exploit graphene for these applications, several synthesis routes, e.g. mechanical[13] and chemical[14] exfoliation, epitaxial growth on silicon carbide (SiC),[15] and chemical vapor deposition (CVD),[16,17] have been employed. Furthermore, realization of these applications to an industrial level requires large scale growth of high quality graphene but many of the synthesis routes listed above have their own advantages and limitations. Until now, mass production of high quality and large area mono to few layers graphene has mainly been achieved by epitaxial growth on single crystal silicon carbide (SiC)[15] and chemical vapor deposition[17] on transition metal substrates such as copper (Cu),[17] nickel (Ni),[18,19] platinum (Pt),[20] etc.

For large area and high quality mono crystal graphene growth, it is very important to control the nucleation density and growth of graphene during the chemical vapor deposition process.[17,21−24] Therefore, much attention has been paid to study the parameters effecting the growth of graphene with emphasis on carbon precursors, hydrogen, catalyst substrate, temperature, and pressure. Graphene films with desirable quality have been grown by optimizing the C:H ratio,[25] using different hydrocarbon[26] and hydrogen gas partial pressures,[25] and smoothing the catalyst substrates by annealing before growth.[27,28] However, the growth results (i.e., domain size, shape, and film quality of the graphene film) vary from one laboratory to another; therefore such wide variations suggest that crucial growth parameters still remain unknown or uncontrolled.

It is a common observation that during the CVD growth of graphene hydrogen plays a vital role on the Cu catalyst substrate. Several previous studies report that during CVD growth of graphene, hydrogen serves a dual role: first, in activation of surface bound active carbon species which play a role for single layer graphene growth, and second, as etching reagent, subsequently controlling the morphology of the graphene domains.[26,29] As on the clean Cu surfaces, molecular hydrogen neither dissociates or adsorbs[30] and therefore its dual role to act as growth activator and etching agent appears to be contradictory. It is established study that group XI metals having filled d-levels are not versatile catalysts for hydrogenation because such metals fail to activation in hydrogen chemisorption.[30] Therefore, one may question that etching of graphene might be caused by the presence of oxygen impurities inside hydrogen gas. There is a recent report stating that graphene etching in hydrogen is caused by trace amounts of oxygen in the hydrogen gas source rather than the hydrogen itself.[31] Furthermore, it has been studied that

Received: October 7, 2014
Revised: January 17, 2015
Published: January 19, 2015

DOI: 10.1021/jp510106w
J. Phys. Chem. C 2015, 119, 3079−3089

oxygen (O) on Cu catalyst surface passivates active sites on its surface, and subsequently suppresses graphene nucleation density,[32] and it has been proposed that oxygen-containing carbon groups could have a role in speeding up graphene growth via the temporary formation of a Cu_2O layer.[33] There are several studies on graphene growth using alcoholic (i.e., methanol, ethanol, and propanol) and other liquid precursors on growth speed and quality of graphene film.[33−35] Such liquid precursors having oxygen containing functional groups could play a critical role in fast and high quality growth of graphene. The graphene growth rate when using ethanol as precursor might be quicker than that of other hydrocarbon precursors,[33] which might be due to the presence of oxygen containing functional groups in the gas mixture during the reaction phase. As a weak oxidant, water vapors may cause oxidation effects easily on the defects and disorders in the graphene sheet. Water has been extensively used as a weak oxidant for etching amorphous carbon in hot atmosphere to achieve the fast and clean growth of single-walled or few-walled carbon nanotubes.[36−38] To the best of our knowledge, there is no report on water assisted growth of graphene or study of the effect of water vapors during CVD growth of graphene on Cu catalyst using methane gas as the carbon source.

In the current work, we have selected water vapors to inspect its effect on graphene growth rate and graphene etching, which results in variation of thickness and morphology of grown graphene using ambient pressure chemical vapor deposition (APCVD). Introduction of water vapors during the growth stage speeds up the growth rate thus increasing the thickness of graphene. Moreover, it also etches the graphene film, consequently resulting in growth of discontinuous microsize multilayer graphene (MLG) islands. To compare the effect of water with hydrogen partial pressure, the growth of graphene under higher hydrogen mass flow rates was also performed, which results in a similar increase in thickness of the graphene film. However, graphene grown under higher hydrogen partial pressure possesses different surface morphology, i.e. continuous MLG film which possesses relatively higher nucleation density.

2. EXPERIMENTAL METHOD

Large area bilayer graphene (BLG) was synthesized on copper foils of 25 um thickness and 99.8% purity (purchased from Alfa Aesar, Cat#46365). APCVD growth technique was employed to synthesize graphene and study the effect of water vapors on its growth. The surface of Cu foil contains surface impurity oxides and oily contaminants, which could be left during its manufacturing process. Therefore, Cu foil was cleaned by ultrasonication in acetone solution for 10 to 15 min followed by drying under nitrogen gas environment. Before heating was started in the quartz tube, Ar and H_2 gas were introduced to dry the lines and lower the humidity level to lower than 150 ppmv and then the quartz tube was evacuated to 0.01 (1×10^{-2}) Pa pressure to remove oxygen. The pressure inside the chamber was raised to atmospheric pressure by introduction of H_2/Ar (600:300 sccm) gases and the tube was heated from room temperature to 1050 °C at a rate of 17 deg/min. Cu foil was annealed at 1050 °C for about 20 min under the same H_2/Ar protection environment and the tube was allowed to cool to reaction temperature, i.e. 1010 °C. The gas flow rates were changed to new values (H_2:Ar with 10:1000 sccm) during the cooling period. At the start of the reaction stage, the reaction gaseous mixture Ar:H_2:CH_4 with flow rates of 1000:10:10 sccm was introduced into the CVD tube. The reaction lasted for 15 min and the tube was cooled to room temperature under Ar:H_2 environment. This condition is referred to as the G1 growth condition (G1 graphene).

Three series of experiments were carried out to compare the effect of water vapors and hydrogen partial pressure on the CVD growth of graphene. For the first series, using optimized conditions for BLG (G1 growth conditions), different water vapor contents, i.e. 500, 750, 1000, 1250, 1500, and 2000 ppmv, were introduced during the reaction stage and thus graphenes grown under these conditions are referred to as GW1, GW2, GW3, GW4, GW5, and GW6, respectively (Table1).

Table 1. Growth Conditions Used for Different Graphene Growth experiments

	CVD growth stage	
sample name	Ar:H_2:CH_4 (sccm)	H_2O vapor (ppmv)
G1	1000:10:10	
GW1	1000:10:10	500
GW2	1000:10:10	750
GW3	1000:10:10	1000
GW4	1000:10:10	1250
GW5	1000:10:10	1500
GW6	1000:10:10	2000
GS1	1000:10:10	
GWS1	1000:10:10	500
GWS2	1000:10:10	750
GWT	1000:10:02	–[a]
GH1	1000:100:10	
GH2	1000:200:10	
GH3	1000:300:10	
GH4	1000:400:10	

[a]500 ppmv water vapor was exposed to Cu catalyst for 6 min just before annealing stage at 1040 °C.

To further investigate the growth mechanism and etching behavior of water assisted graphene growth, a series of short time growth experiments were performed with four different growth conditions. In the first growth experiment, we used the G1 growth condition for just 1 min and 50 s growth time; as a result the catalyst surface was fully covered with continuous single layer graphene (referred to as GS1 graphene). For the second and third experiments, 500 and 750 ppmv water vapors were introduced using the GS1 condition, and as a result discontinuous graphene islands were grown, therefore referred to as GWS1 and GWS2 graphene, respectively. For the final short time graphene growth experiment, we treated Cu foil with water vapors exposure for 6 min at 1040 °C, just before the annealing stage. After treatment, Cu foil was annealed under Ar/H gases for an hour and exposed to the reaction gases mixture (Ar/H/CH_4, with 2 sccm methane flow rate) for 1 min and 50 s, thus referred to as GWT graphene. This resulted in six membered flower type distinct graphene grains.

For the third series of experiments, optimized G1 growth condition was used with H_2 gas mass flow rate varying from 100, 200, 300, and 400 sccm during the reaction stage; therefore, graphenes grown under these conditions are referred to as GH1, GH2, GH3, and GH4 graphene, respectively. It is observed that the thickness of the graphene film increases with an increase in hydrogen partial pressure during the reaction stage, but graphene grown under higher hydrogen partial pressure is continuous relative to porous and discontinuous graphene islands grown under water vapor environments. The method to transfer

DOI: 10.1021/jp510106w
J. Phys. Chem. C 2015, 119, 3079−3089

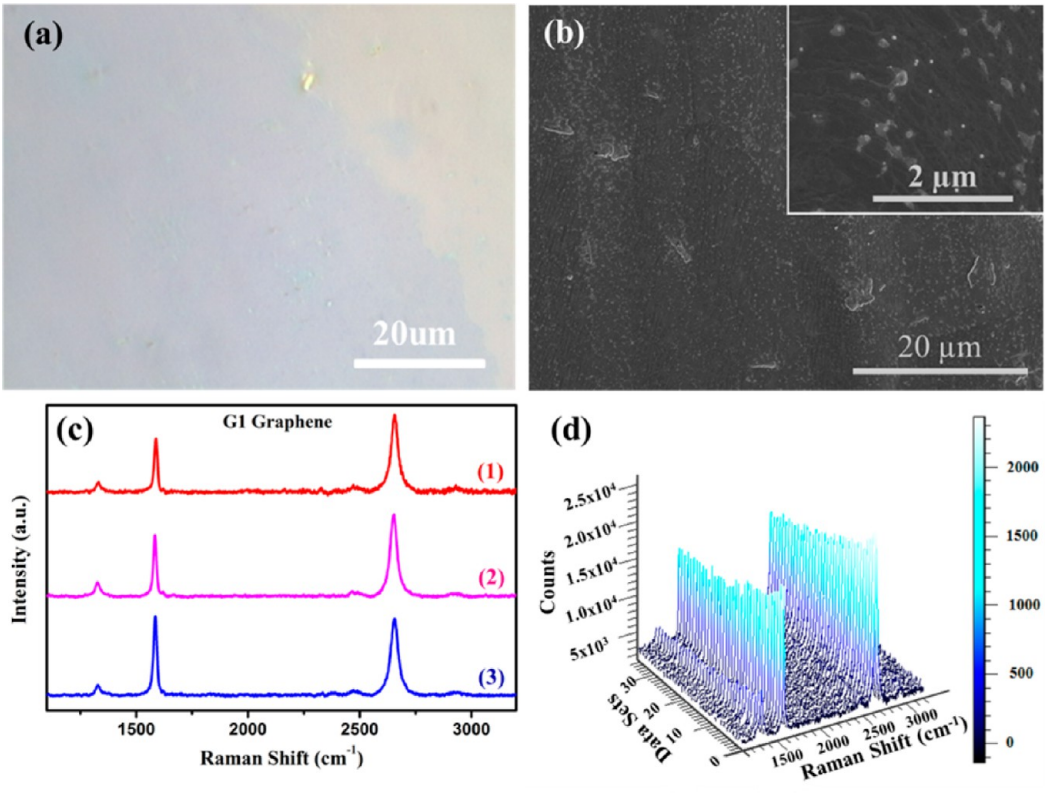

Figure 1. G1 graphene film: (a) optical image of graphene film transferred on Si/SiO_2 substrate, (b) SEM micrograph of G1 graphene on Cu foil (where inset is image taken at high magnification), (c) Raman spectra of graphene at different points, and (d) 3D Raman mapping for D, G, and 2D band intensities.

graphene on arbitrary substrates is described in the Supporting Information.

The structural characterization of CVD grown graphene under different conditions was carried out with a field emission scanning electron microscope (FE-SEM, NOVA NanoSEM 450), Raman spectroscope (Renishawin Via plus, operated at 632.8 nm, He−Ne laser, 4.0 mW laser power, 50× objective lens), and transmission electron microscope (TEM, FEI Tecnai G220 S-Twin, operated at 200 kV). An ultraviolet−visible spectrometer (Jasco V-550) was used for transmittance measurements for graphene grown under different growth conditions.

3. RESULTS AND DISCUSSION

Graphene growth using the CVD process is divided into four steps: dissociation of hydrocarbon gas molecules, diffusion of active carbon species on the catalyst surface, formation of graphene nucleation islands, and growth of graphene islands to merge into complete graphene film.[39] Under optimized conditions, BLG (referred to as G1 graphene) with a continuous background of mono layer graphene was synthesized by APCVD.

The optical microscopic study of G1 graphene transferred on Si/SiO2 substrate illustrates a continuous graphene film with full coverage on the catalyst substrate, as shown in Figure 1a. The field emission scanning electron microscope (FESEM) study shows that G1 graphene is a continuous single layer of which more than 85% area is covered by secondary layer graphene domains (Figure 1b). Raman spectra taken from three different points and Raman surface mapping of G1 graphene, transferred on SiO_2 substrate is shown in Figure 1c,d. The intensity ratio of the 2D to G band (I_{2D}/I_G) for the first and second Raman spectra of G1 graphene is greater than one (Figure 1c), whereas the intensity ratio I_{2D}/I_G for the Raman spectra taken from the third spot of G1 graphene is equal to one. The measured intensity ratio of the 2D to G band (I_{2D}/I_G) for the first, second, and third Raman spectra of G1 graphene are 1.32, 1.25, and 0.99, whereas intensity ratios for the D to G band (I_D/I_G) are 0.21, 0.26, and 0.18, respectively. This indicates growth of a continuous single layer G1 graphene sheet with random second layer grains on its surface.

The Raman spectra of G1 graphene own a very small D band signifying low grain boundary crystal defects. Moreover, some defects may also arise during the graphene transfer process. To confirm the continuity of the graphene film, Raman surface mapping was performed, as indicated in Figure 1d. The continuous intensity ratios of D, G, and 2D bands confirm the continuity of G1 graphene.

3.1. Effect of Water Vapors. *3.1.1. Effect of Water Vapors for Long Time Growth.* Although the quality of G1 graphene is not best as reported in the literature, however this condition was taken as reference to study the effect of water vapor contents on the APCVD growth of graphene (referred to as GW1, GW2, etc.). The water vapor assisted growth of multilayer graphene was performed by introducing water vapor contents during the growth stage by keeping all other parameters similar to the G1 growth condition. Figure 2a shows the Raman spectra of MLG for graphene grown under GW1 to GW6 growth conditions (as given in Table 1). The intensity ratio of the 2D to G band (I_{2D}/I_G) for Raman spectra of GW1 graphene transferred on Si/SiO_2 substrate is nearly equal to one (i.e., 0.96), thus indicating the growth of BLG film. The second Raman spectra is taken from graphene grown under GW2 condition, for which the intensity ratio of the 2D to G band (I_{2D}/I_G) is around 0.79, thus indicating 3 to 4 layers of graphene.

DOI: 10.1021/jp510106w
J. Phys. Chem. C 2015, 119, 3079−3089

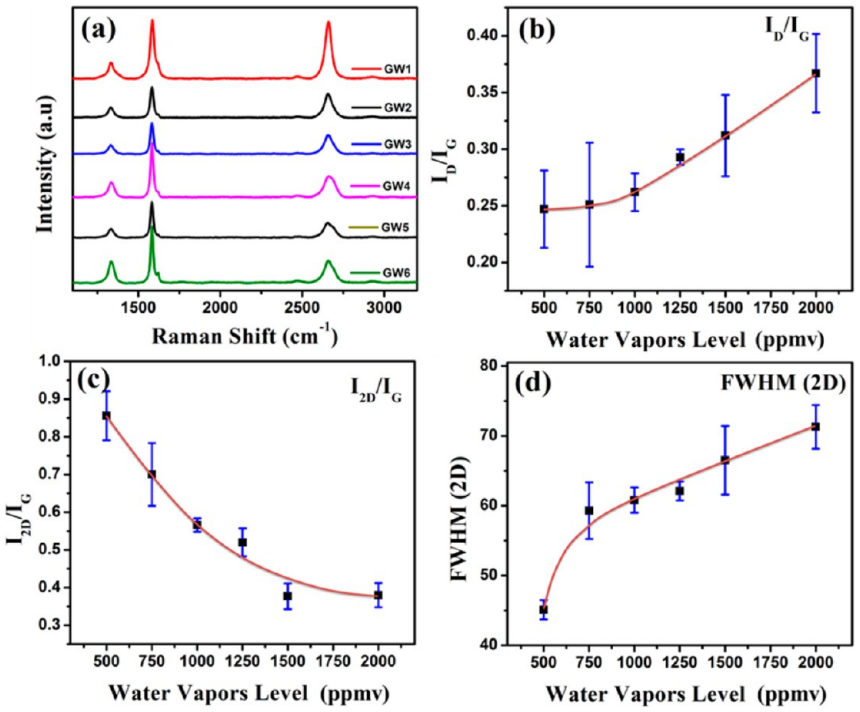

Figure 2. Effect of water vapors: (a) Raman spectra of graphene grown under GW1, GW2, GW3, GW4, GW5, and GW6 growth conditions, (b–d) statistical distributions of average values of I_D/I_G, I_{2D}/I_G, and FWHM for the 2D band of graphene grown under different water vapor assisted growth conditions (15 data sets were taken for each sample).

The 2D to G band intensity ratio (I_{2D}/I_G) for the GW3 graphene sheet is observed to be 0.61 indicating growth of MLG; however, the number of graphene layers cannot be exactly determined from the Raman spectra. Similarly for GW4 and GW5 graphene sheets, the intensity ratios of the 2D to G band (I_{2D}/I_G) are approximately equal to 0.44 and 0.41, respectively (as shown in Figure 2a). The intensity ratio of the 2D to G band (I_{2D}/I_G) for graphene sheets grown under GW6 condition is around 0.37. However, the G band for the GW6 graphene sheet is quite similar to that for graphite, with an additional band near the G band at 1620 cm^{-1}; therefore, we can estimate the thickness of the GW6 graphene sheet to be more than 20 layers. The statistical distribution of average values of I_D/I_G, I_{2D}/I_G, and FWHM is illustrated in Figure 2b–d, where the error bars represent standard deviation against specific growth condition. The average values (of I_D/I_G, I_{2D}/I_G, and FWHM) and standard deviations are taken from 15 data sets for each sample.

The average D to G band intensity ratios (I_D/I_G) for water assisted grown graphene sheets (i.e., GW1 to GW6) are 0.24, 0.25, 0.26, 0.29, 0.31, and 0.38, respectively. Moreover, the theoretically calculated grain size[33] corresponding to I_D/I_G intensity ratios for G1 graphene is 1.82 μm, and for water assisted grown graphene are 1.59, 1.53, 1.47, 1.32, 1.24, and 1.08 μm, respectively. These findings indicate significant increase in the D band value, thus quality of water assisted MLG sheets does not remain the same as that of G1 graphene. Therefore, it can be concluded that by introducing water vapors during the growth stage in the APCVD process, MLG domains can be synthesized with significant compromise on the quality of graphene. Figure 2c,d reflects the decreasing trend in I_{2D}/I_G ratio and increasing trend in FWHM with rise in water vapor contents, therefore signifying an increase in graphene thickness.

FESEM was used to study the surface morphology and continuity of graphene grown under different growth conditions. Figure 3 illustrates the effect of water vapors on thickness and morphology of GW1, GW2, GW3, GW4, GW5, and GW6 graphene. It is obvious from FESEM micrographs that by increasing water vapor contents, MLG domains are grown over a continuous range on the Cu catalyst surface. Moreover, the size of graphitic islands decreases but their thickness increases with increase in water vapor contents.

Large area surface morphology of multilayer graphene islands on copper catalyst substrate grown under different water vapor conditions is shown in the highly magnified FESEM micrographs of Figure S.1, Supporting Information. The size range of graphitic islands of GW1, GW2, GW3, GW4, GW5, and GW6 graphene is 2.0–5.0, 2.0–3.0, 0.5–1.0, 0.3–1.0, 1.0–2.0, and 0.15–0.8 μm, respectively. Therefore, it might be concluded that water vapors play a double role; (1) due to the presence of an oxygen-containing functional group, water molecules etch amorphous carbon and graphene edges,[31] which may facilitate active carbon atom diffusion under the grown graphene domains, subsequently increasing the number of graphene layers; (2) water itself and oxygen-containing carbon groups produced during the etching process could have a role in speeding up graphene growth via the temporary formation of a Cu_2O layer.[33]

To support the Raman results and further investigate the effect of water vapor on the thickness of graphene sheets, a TEM study was performed. Graphene film was transferred on Cu gate containing amorphous carbon film with microsize holes. Figure 4 illustrates the TEM images of graphene grown under different growth conditions, without water, i.e. G1 growth condition, and with water vapors, i.e. GW2, GW3, GW4, GW5, and GW6 growth conditions. Figure 4a illustrates the TEM micrograph of G1 graphene film synthesized without the assistance of water vapors, where the single layer edge of the G1 graphene film can be clearly observed from the inset. This confirms the single layer nature of G1 graphene which contains secondary layer grains, as

DOI: 10.1021/jp510106w
J. Phys. Chem. C 2015, 119, 3079–3089

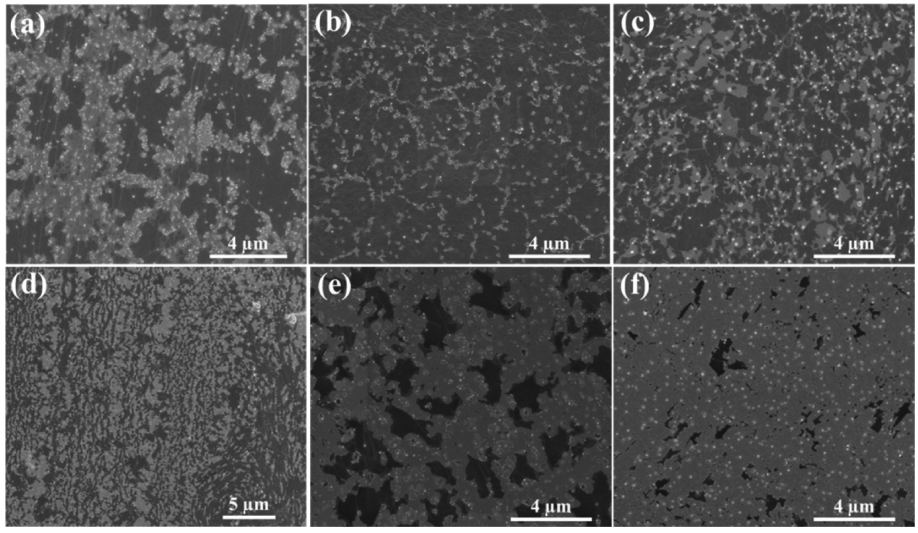

Figure 3. Effect of water vapors on surface morphology of graphene sheets: FESEM images of (a) GW1, (b) GW2, (c) GW3, (d) GW4, (e) GW5, and (f) GW6 graphene grown under 500, 750, 1000, 1250, 1500, and 2000 ppmv water vapor contents, respectively.

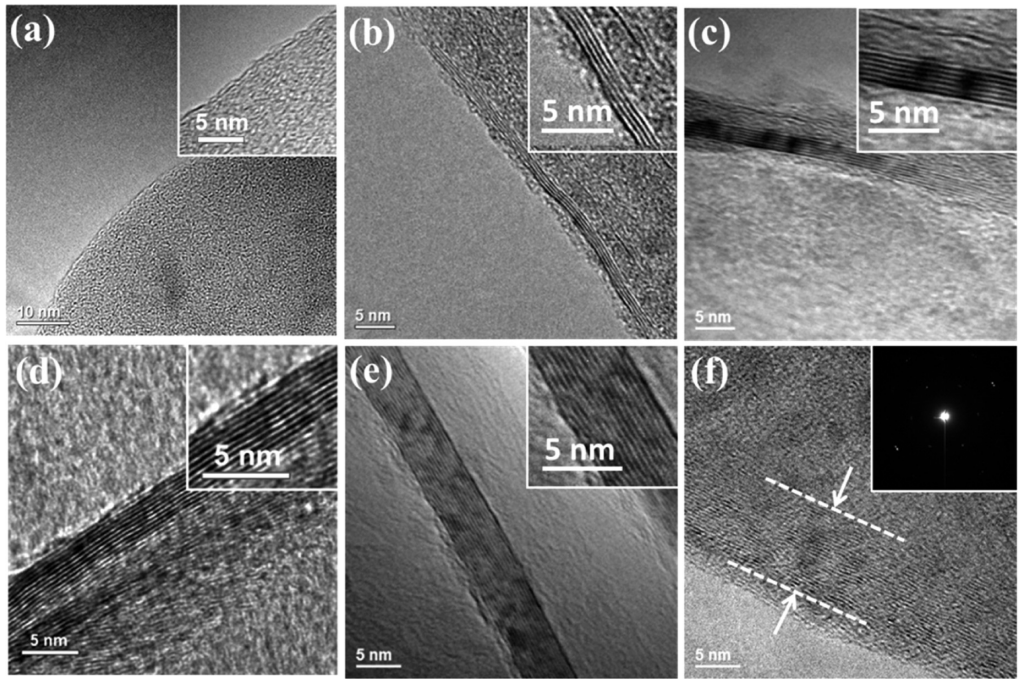

Figure 4. Effect of water vapors on thickness of graphene sheets: TEM images of (a) G1 (without water), (b) GW2, (c) GW3, (d) GW4, (e) GW5, and (f) GW6 grown graphene edges. The insets in panels a−e are the magnified TEM images for the edge of the respective graphene sheets, whereas the inset in panel f is the electron diffraction pattern of GW6 graphene.

observed in SEM results. Figure 4b elucidates the 4 layer graphene edge grown under the GW2 growth condition; thus the thickness of the GW2 graphene sheet as confirmed by TEM analysis varies from 3 to 4 layers. The thickness of the graphene sheet grown under the GW3 condition is confirmed to be around 8 to 9 layers (as shown in Figure 4c), whereas the graphene grown under the GW4 condition is comprised of 11 to 12 layers, as observed in Figure 4d. The GW5 grown graphene under 1500 ppmv water vapor concentration is observed to be 15 layer thick (Figure 4e). The insets in Figure 4a−e are magnified images of the edge of the corresponding graphene samples. When the water vapor contents were increased to 2000 ppmv (i.e., GW6 growth condition), graphitic sheets was obtained comprised of 22 to 25 layers (Figure 4f). The inset in Figure 4f exhibits the electron diffraction pattern of thick layer graphite grown under the GW6 growth condition. The TEM results for graphene sheets grown under different water vapor exposures (i.e., GW1 to GW6 graphene) are consistent with Raman spectroscopy results. From TEM and Raman studies, it is observed that increasing water vapor concentration causes an increase in growth rate, subsequently increasing the thickness of graphene layers; however, FESEM analysis revealed the strong etching of graphene caused by water vapors, therefore resulting in the growth of discontinuous graphene islands.

It is clear from Raman spectroscopy and TEM analysis that by increasing the water vapor content level, the thickness of the

DOI: 10.1021/jp510106w
J. Phys. Chem. C 2015, 119, 3079−3089

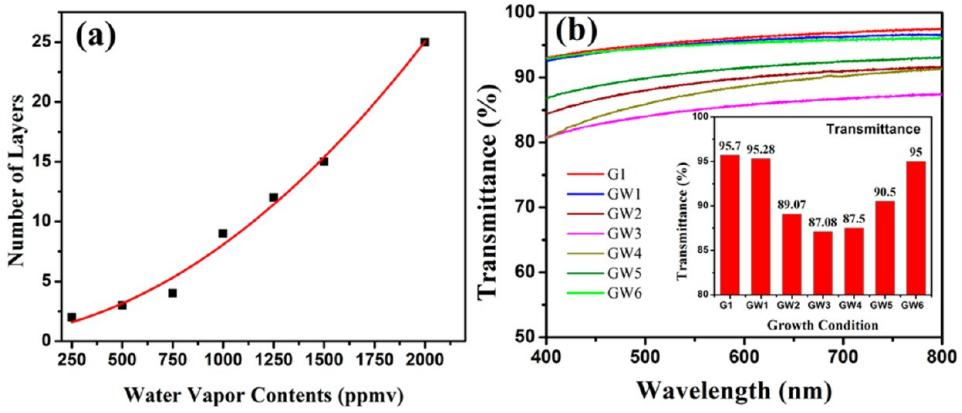

Figure 5. (a) Plot for the number of graphene layers vs water vapor contents; (b) UV−vis spectroscopy curve plots for transmittance of G1, and GW1−GW6 graphene, whereas the inset is the column plot of transmittance (%) for graphene grown under different growth conditions (transmittance is measured at 550 nm).

graphene film increases from BLG to MLG. Figure 5a shows a plot of the number of graphene layers with the water vapor contents (ppmv), which illustrates that the thickness of graphene sheets increases exponentially with the rise in water vapor concentration introduced during the growth stage of the CVD process. To further investigate the thickness of graphene sheets grown under different growth conditions (G1, GW1−GW6), UV−vis spectroscopy analysis was performed.

Figure 5b illustrates the UV−vis transmittance (%) curves for graphene films grown under different growth conditions, and the inset is the column plot of the transmittance (%) for G1, and GW1−GW6 growth conditions. Transmittance initially decreases from 95.7% (250 ppmv, G1 growth condition) to 87.08% (1000 ppmv, GW3 growth condition) with an increase in water vapor concentrations up to 1000 ppmv. However, with further increase in water vapor contents, transmittance increases to 95.0% for the GW6 growth condition. The reason for this discrepancy was only because of the decrease in coverage area of multilayer graphene gains, as discussed during SEM analysis (Figure 3).

3.1.2. Effect of Water for Short Time Growth. To further investigate the growth mechanism and etching behavior of water, short time graphene growth was also performed. Figure 6 illustrates the short time growth of graphene with and without water vapors. Figure 6a represents the FESEM micrograph for graphene grown without water vapors (GS1 growth condition, as shown in Table 1). It is obvious from the SEM results that the Cu surface is completely covered with graphene film and some darker islands are also visible, thus suggesting secondary nucleation already took place, even though growth time was less than 2 min. Some graphene tears can also be observed on its surface, which are clearly visible in the inset of Figure 6a. This elucidates that although the catalyst surface was fully covered with graphene, yet growth time was not enough to fill tears of the graphene film. From the comparison of GS1 and G1 growth results, it can be observed that growth of the single layer graphene is much faster (less than 2 min, i.e. GS1) than that of the secondary layer graphene which took 15 min to cover 85% area (i.e., G1 graphene). Figure 6b,c shows the FESEM micrographs for water vapor assisted grown graphene for short time, with different water vapor concentrations (GWS1 and GWS2 growth conditions). SEM results of water assisted graphene growth for short time (i.e., GWS1 and GWS2) clearly revealed the strong etching effect caused by water vapors. It is

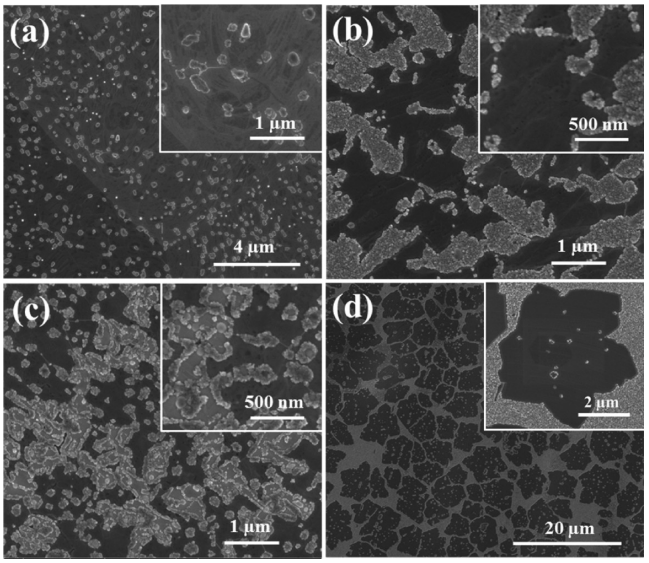

Figure 6. SEM images for short time growth of graphene: (a) without water (GS1), (b and c) with water vapors 500 ppmv (GWS1) and 750 ppmv (GWS2), respectively; and (d) GWT graphene grown on water treated Cu foil. The insets in the micrographs are the high magnification images for the respective graphene samples.

obvious from results that etching propagates along wrinkles in the graphene film. Furthermore, the graphene islands reduce in size with an increase in water vapor concentration, i.e. the size of the GWS2 graphene islands (750 ppmv, Figure 6c) is smaller than that of GWS1 (500 ppmv, Figure 6b), signifying that the higher the water vapor concentration the faster the etching rate. It is obvious from the insets of Figure 6b,c that very small secondary layer graphene grains are present on graphene islands, which are larger in size but fewer in number for GWS2 graphene relative to GWS1. Thus, this indicates the faster graphene growth rate and suppression in nucleation density for higher water vapor concentration. Although higher water vapor results in a fast etching rate as well, the etching effect is propagating from the boundary/edges of graphene islands, therefore it may not affect the small secondary grains on primary graphene islands.

To further understand the effect of water vapors on Cu catalyst, we performed graphene growth for a short time on a water vapor treated Cu foil (GWT growth condition, as shown in Table 1). After water vapor treatment of Cu foil, it was annealed

DOI: 10.1021/jp510106w
J. Phys. Chem. C 2015, 119, 3079−3089

for an hour under hydrogen and Ar atmosphere. Cu foil was partially oxidized by water vapor treatment at high temperature, which might react on active sites and defects on its surface. Then, it was annealed under hydrogen−argon atmosphere which cleaned partially oxidized areas by dehydrogenation. Due to the presence of surface oxygen as a result of water vapor treatment, very less active sites remain available for graphene nucleation, and therefore resulting in suppression of graphene nucleation density[32] (as illustrated in Figure 6d), as well as this surface oxygen causing an increase in graphene growth rate.[32] It is obvious from the SEM micrograph that separate six corner, flower type graphene grains grew, which could be due to etching of graphene caused by surface oxygen[32] left on active sites because of water treatment. The secondary layer graphene grain is perfectly hexagonal in shape, which clearly distinguishes the strong etching of the primary layer relative to the secondary layer graphene. The size of the primary layer graphene grain ranges from 4 to 5 μm, whereas the secondary layer domain is around 1 μm.

3.2. Effect of Hydrogen. To study the effect of hydrogen gas partial pressure for comparison with the effect of water vapors on thickness and morphology of graphene, growth was performed by using G1 growth conditions as reference and varying the mass flow rate of hydrogen gas during the reaction stage of the CVD process. The graphenes grown under different hydrogen mass flow rates, i.e. 100, 200, 300, and 400 sccm, are referred to as GH1, GH2, GH3, and GH4, respectively (as shown in Table 1).

FESEM micrographs for GH2 and GH4 grown graphene films are shown in Figure 7a,b. It is clear from the FESEM micrograph

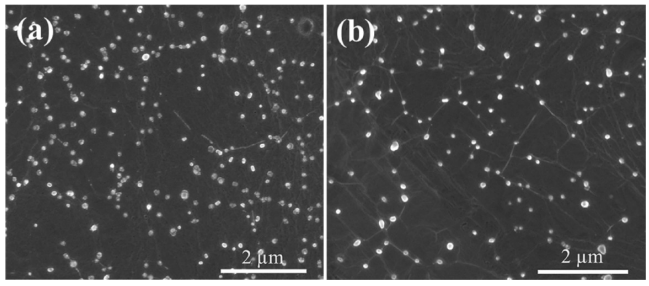

Figure 7. Effect of hydgrogen: (a) GH2, and (b) GH4 grown graphene films under 200 and 400 sccm H_2 gas mass flow rate, respectively.

of GH2 graphene that the graphene film is continuous with multilayer grains and its surface does not look very uniform. Furthermore, it is clear from the FESEM image that GH4 graphene is composed of a continuous multilayer graphene film. It is important to note that the continuity of the GH4 graphene film appears to be more than that of the GH2 graphene film, which demonstrates that high hydrogen concentration causes growth of continuous graphene film by merging the secondary layer graphene domains. The carbon particles can be observed on the surface of samples which might deposit during sample preparation for SEM characterization.

Moreover, it can be observed that GH4 graphene film possesses more wrinkles on its surface, which appear during cooling after CVD growth due to the difference in coefficient of thermal expansion of graphene and Cu substrate.[40] Thus, these wrinkles indicate the continuous nature of the GH4 graphene film.

To further investigate the effect on graphene films grown under different hydrogen flow rates, Raman spectroscopy and TEM characterizations have been performed. The intensity ratio of the 2D to G band (I_{2D}/I_G) for Raman spectra of the GH1 graphene sheet transferred on Si/SiO_2 substrate is nearly equal to one (i.e., 1.10), thus indicating growth of double layer graphene (as shown in Figure 8a). The second spectra in Figure 8a illustrates the Raman spectra of the graphene film grown under GH2 condition, for which the intensity ratio of the 2D to G band (I_{2D}/I_G) is around 0.74, thus signifying growth of 4 to 5 layers thick graphene film. The 2D to G band intensity ratio (I_{2D}/I_G) for the GH3 graphene sheet is observed to be 0.61 demonstrating few layer graphene sheets, but the number of graphene layers cannot be exactly determined from the Raman spectra.

Similarly for the GH4 graphene film, the intensity ratio of the 2D to G band (I_{2D}/I_G) is approximately equal to 0.52. On the other hand the D to G band intensity ratio (I_D/I_G) for graphene grown under different hydrogen flow rates (i.e., GH1 to GH4) is higher than that of water assisted grown graphene. Figure 8b−d exhibits the statistical distribution for average values of I_D/I_G, I_{2D}/I_G, and FWHM of Raman spectra taken from graphene grown under different hydrogen flow rates. Figure 8b illustrates the variation in I_D/I_G ratio with increase in hydrogen flow rate, due to higher nucleation density. The average values of the I_D/I_G ratio for GH1 to GH4 are 0.23, 0.31, 0.44, and 0.36, respectively. The average I_D/I_G ratio for GH3 growth condition is observed maximum. Therefore, we can conclude that for water vapors assisted growth of multilayer graphene film, the quality degrades less with respect to that of graphene film grown under high hydrogen partial pressure. The average values for I_{2D}/I_G decrease and FWHM increase exponentially by increasing hydrogen partial pressure (as shown in Figure 8c,d), thus indicating increase in graphene film thickness.

Furthermore, TEM study was performed to analyze surface morphology and thickness of graphene grown under the GH2 growth condition. The graphene film was transferred on Cu gate containing carbon film with microsize holes. Figure 8e illustrates high magnification TEM images of GH2 graphene sheets, where the inset is the magnified image of the edge of the graphene sheet. GH2 graphene sheets are continuous with multilayer grains comprised of 5 to 6 layers. It might be concluded that the thickness of the graphene film increases with an increase in the H_2:CH_4 ratio, i.e. at high hydrogen partial pressure, the molecular oxygen present in hydrogen gas as trace impurities can etch weakly bonded carbon atoms from graphene edges.[31] Therefore, it creates sites for active carbon species to reach the catalyst surface and may result in double layer or multilayer graphene. Moreover, the presence of oxygen impurities in hydrogen gas may also increase the growth rate by partially oxidizing the Cu catalyst surface,[33] which results in multilayer graphene.

3.3. Growth Mechanism. *3.3.1. Water Assisted Graphene Growth Mechanism.* From the results discussed above, it has been observed that graphene growth rate is very high when using water vapors along with methane precursor during the reaction stage and some insight into the chemistry of growth can be inferred. To investigate the CVD growth mechanism and the graphene growth rate, several studies have been carried out using different growth conditions and different precursors. Li et al. have reported that complete coverage of the Cu catalyst with single layer graphene can be achieved in 2 min using methane as precursor gas, with a flow rate of 7 sccm at 1035 °C.[41] Similarly, during our short time growth experiment (GS1 graphene), full catalyst coverage with continuous single layer graphene film has been achieved in less than 2 min (i.e., 1 min and 50 s). The minimum growth time for complete coverage of Cu foil, when using ethylene (C_2H_4) as the carbon precursor, has been reported to be 5 min, which is comparable to CH_4.[42] In the case

DOI: 10.1021/jp510106w
J. Phys. Chem. C 2015, 119, 3079−3089

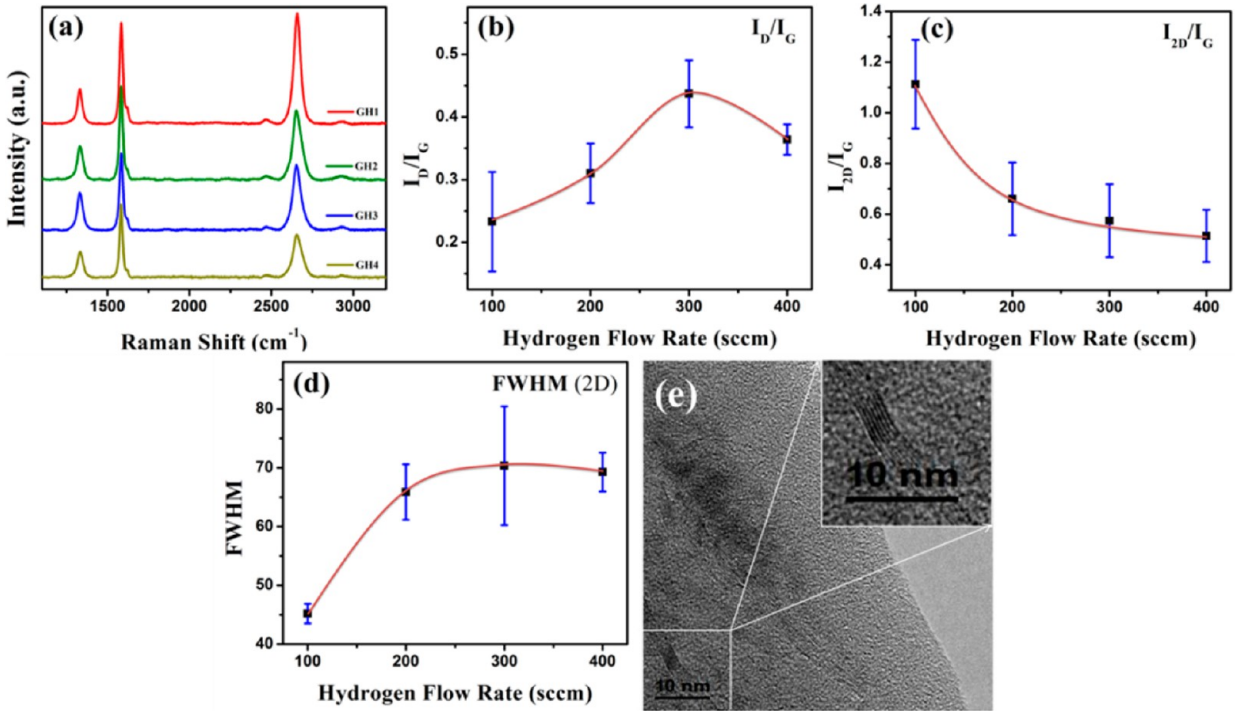

Figure 8. Effect of hydrogen gas flow rate on thickness of graphene sheets: (a) Raman spectra of GH1, GH2, GH3, and GH4 graphene, (b–d) statistical distributions of average values of I_D/I_G, I_{2D}/I_G, and FWHM of Raman spectra for graphene grown under different hydrogen mass flow rates (15 data sets are taken for each sample), and (e) TEM image of GH2 graphene sheets, where the inset is the magnified image of the GH2 graphene edge.

of other liquid precursors, the minimum growth time reported for the complete coverage of catalyst surface with continuous graphene film is longer than that for CH_4, i.e. 4 min for *n*-hexane,[43] 15 min for benzene,[44] and 60 min for toluene.[45]

There are several reports on growth rate and quality of graphene film,[33−35] using ethanol as precursor. The graphene growth using ethanol precursor is much faster than that of other hydrocarbon precursors. In a recent report, polycrystalline single layer graphene film was grown on complete Cu catalyst surface in just 20 s.[33] There is a correlation between graphene growth using water vapors (used along with methane precursor) and ethanol; both contain oxygen which might play a critical role in growth rate as well as etching, during the CVD growth of graphene. It is well-known that ethanol undergoes thermal pyrolysis under high temperature. One of the possible paths for thermal decomposition of ethanol may result in the formation of ethylene along with water, while another route leads to formation of hydrogenated and oxygen containing carbon groups.[46] In either case, the presence of oxygen containing molecules during the CVD process can positively influence the growth of graphene film by etching amorphous carbon and removing defects, as happened in the case of water assisted growth of CNTs.[37] However, the presence of oxygen molecules even in trace quantities can lead to etching of graphene film;[31] as in our case, strong graphene etching was observed during water vapor assisted growth of graphene (Figures 3 and 6b,c). As a weak oxidant, the oxidation effect of H_2O may easily occur at the defects and disorders. Water vapors cause the etching of amorphous carbon and weakly bounded carbon atoms near the graphene boundary.[38] The oxidation of amorphous carbon and weakly bound carbon on graphene edges with water vapors at high temperature can produce H_2 and CO molecules.[38]

$$C + H_2O \rightarrow CO + H_2 \quad (1)$$

$$\text{graphene} + H_2O \rightarrow (\text{graphene} - C) + CO + H_2 \quad (2)$$

Our results are in agreement with a recent report[31] stating that molecular oxygen present in the hydrogen causes graphene etching instead of hydrogen itself, thus it contradicts the previous reports stating that hydrogen is responsible for etching of graphene.[26,29] Moreover, the role of water and oxygen should be further investigated as it also plays a role in increasing growth rate, which results in growth of multilayer graphene. During the interaction of methane with oxidized Cu at high temperature, adsorption of carbon radicals on the oxidized Cu surface is much quicker relative to that of clean Cu surface;[47] likewise, it is also reported that thermal decomposition of methanol on partially oxidized Cu surface is more efficient relative to clean Cu surface.[48] Moreover, water treated Cu foil may retain surface oxygen which suppresses graphene nucleation density, and may also increase growth rate,[32] as shown in Figure 6d. The amount of CO released during the etching of graphene or amorphous carbon as well as water introduced during CVD growth could induce formation of a temporary layer of Cu_2O on the Cu surface, while free hydrogen atoms instantly reduce the Cu_2O layer.[33] Therefore, adsorption of active carbon species could be improved due to the oxidation/dehydrogenation reaction,[47] thus leading to rapid growth of the graphene film. The water assisted multilayer graphene might be highly rich in oxygen functional group contents relative to strongly oxidized acid treated graphene, as happened in the case of CNTs.[36] This rough surface, rich in oxygen functional groups, can be helpful for loading nanoparticles.

3.3.2. Modified Graphene Growth Mechanism: Catalytic Role of Hydrogen. The CVD growth of graphene is strongly influenced by hydrogen when using methane as the carbon source and Cu foil as the catalyst. During the CVD growth of graphene, hydrogen serves a dual role: first, in activation of

DOI: 10.1021/jp510106w
J. Phys. Chem. C 2015, 119, 3079−3089

surface bound active carbon species which play a role for single layer graphene growth,[26] and second, as carrier gas containing oxygen impurities as etching reagent,[31] subsequently controlling the morphology of the graphene domains. The presence of oxygen impurities in hydrogen gas may also affect the growth rate by partially oxidizing the Cu catalyst surface,[33] as discussed in the above section. For constant methane gas flow, the growth rate varies with hydrogen partial pressure and is maximum at a hydrogen pressure 200−400 times that of methane gas.

It has been studied that low hydrogen pressure (hence carrying less etching impurities) results in nonpassivation of graphene edges, thus firmly stick with the catalyst substrate.[29] This prevents the active carbon species from diffusing under the covered graphene sheet, thus a single layer graphene growth is favored. Contrary to the previous report that high hydrogen pressure tends to terminate the graphene edges,[29] our results suggest that in fact at high hydrogen pressure, the concentration of oxygen impurities becomes significant, thus graphene edges etching becomes a dominant factor.[31] Therefore, it provides a path for diffusion of active carbon species below the top layer of graphene, resulting in growth of bilayer to multilayer graphene.

In comparison to other catalyst substrates, Cu has very low carbon solubility which makes it a preferable substrate for the growth of single layer graphene.[29] Thermodynamically, the chemisorption of methane gas on copper substrate to form surface bound carbon active species $(CH_{x<4})_s$ is unfavorable. However, once the surface bound active carbon is formed, this results in thermodynamically favorable agglomeration into multimeric $(C_nH_y)_s$ species, subsequently leading to multilayer graphitic film.[49] The formation of CH_x has been reported to be less promising in the gas phase and growth of the second (and third) layer graphene is extremely slow when the catalyst surface is already covered with a graphene layer.[50]

The peculiar behavior of hydrogen gas for different partial pressures reflects the complex role during chemical vapor deposition reaction especially when methane is used as the carbon source. In the absence of hydrogen gas in the reaction mixture, surface bound active carbon species $(CH_3, CH_2, CH, C)_s$ are formed through the chemisorbed process on the Cu catalyst substrate which subsequently results in the formation of graphene.[26] However, experimental and density functional theory (DFT) studies have revealed that such dehydrogenation reactions are not thermodynamically favorable even on Cu substrate.[49,51] Such an endothermic process could be the rate limiting step under low methane partial pressure, subsequently obstructing the graphene growth process without an additional catalyst such as hydrogen. Alternatively, graphene growth can be sustained by excessive methane gas flow overcoming unfavorable thermodynamics,[52] but elimination of the second layer graphene is difficult with this route. The scheme of the critical role of hydrogen in graphene growth is illustrated below:[26]

$$Cu + H_2 \leftrightarrow 2H_s \quad (3)$$

$$Cu + CH_4 \rightarrow (CH_3)_s + H_s \text{ (slow)} \quad (4)$$

$$Cu + CH_4 \leftrightarrow (CH_4)_s \quad (5)$$

$$(CH_4)_s + H_s \leftrightarrow (CH_3)_s + H_2 \quad (6)$$

$$(CH_3)_s + \text{graphene} \leftrightarrow (\text{graphene} + C) + H_2 \quad (7)$$

$$O_{2(\text{impurity})} + \text{graphene} \rightarrow (\text{graphene} - C) + CO + H_2O \quad (8)$$

The catalytic role of hydrogen is shown in reactions 3 and 6 for activation of surface bound carbon species. Hydrogen molecules readily dissociate on the catalyst substrate resulting in active hydrogen atoms[53,54] (reaction 3), which in turn activate physisorbed methane molecules (reaction 6), leading to formation of surface bound carbon $(CH_3, CH_2, CH, C)_s$ radicals. These subsequent dehydrogenation steps to generate active carbon radicals are endothermic, but their role can be more critical for graphene growth. The unstable surface bound active carbon $(CH_x)_s$ species aggregates into stable graphene (reaction 7). The high hydrogen partial pressure causes excessive production of active carbon species due to the catalytic role of hydrogen (reaction 6), which may increase the availability of active carbon radicals to absorb on the Cu surface. Moreover, at high hydrogen partial pressure, the molecular oxygen present in hydrogen gas as trace impurities can etch weakly bonded carbon atoms from graphene edges[31] (reaction 8), therefore creating sites for active carbon species to reach the catalyst surface and may result in double layer or multilayer graphene. At high methane partial pressure, growth rate overcomes the etching effect, and subsequently may result in irregular shaped graphene grains.

4. CONCLUSION

From the above results and discussion, we may conclude that the thickness and size of graphene islands can be controlled by water vapor concentration introduced during the reaction stage of the CVD growth process. BLG was synthesized under optimized growth conditions in the absence of water vapors. For water assisted MLG growth, different water vapor concentrations were introduced during the growth stage while keeping all other parameters the same as the G1 growth condition. By increasing the water vapor concentration from 0 to 2000 ppmv, the number of graphene layers increases from 2 to 25 layers. This might be attributed to the dual role of water vapors: (1) etching amorphous carbon and graphene edges, thus providing a path for diffusion of active carbon radicals on the Cu surface for growth of discontinuous MLG islands and (2) partially oxidizing Cu catalyst by formation of a temporary Cu_2O layer that might be immediately reduced by hydrogen atoms, subsequently increasing the growth speed. On the other hand, higher hydrogen partial pressure leads to formation of continuous MLG film. It might be attributed to the (1) catalytic role of hydrogen for dissociation of active carbon radicals and (2) etching of graphene edges as well as partially oxidizing Cu catalyst surface caused by oxygen impurities present in hydrogen gas which might boost growth rate, therefore resulting in the growth of the MLG graphene film. Moreover, at low hydrogen partial pressure (i.e., higher methane partial pressure) growth rate dominates the etching effect caused by oxidizing impurities in hydrogen gas, hence resulting in the growth of single or double layer graphene. From the above results and discussion, it might also be concluded that the etching of graphene at high hydrogen partial pressure is caused by oxygen impurities present in hydrogen gas, rather than hydrogen itself.

■ ASSOCIATED CONTENT

Supporting Information

High magnification FESEM images of GW1 to GW6 graphene and the method to transfer graphene on arbitrary substrates. This material is available free of charge via the Internet at http://pubs.acs.org.

DOI: 10.1021/jp510106w
J. Phys. Chem. C 2015, 119, 3079−3089

AUTHOR INFORMATION

Corresponding Authors

*Fax: +86 411 84709304. E-mail: asifnust86@gmail.com (M.A.).
*Fax: +86 411 84709304. E-mail: lpan@dlut.edu.cn (L.P.).

Notes

The authors declare no competing financial interest.

ACKNOWLEDGMENTS

This work was supported by the National Natural Science Foundation of China (Nos. 61137005 and 11274055) and the Program for Liaoning Excellent Talents in University. Special thanks to Dr. Muhammad Rashad for giving valuable time for discussion of experimental results and for helping us in revising the manuscript.

REFERENCES

(1) Castro Neto, A. H.; Guinea, F.; Peres, N. M. R.; Novoselov, K. S.; Geim, A. K. The Electronic Properties of Graphene. *Rev. Mod. Phys.* **2009**, *81*, 109−162.

(2) Falkovsky, L. A. Optical Properties of Graphene. *J. Phys.: Conf. Ser.* **2008**, *129*, 012004.

(3) Barton, R. A.; Ilic, B.; van der Zande, A. M.; Whitney, W. S.; McEuen, P. L.; Parpia, J. M.; Craighead, H. G. High, Size-Dependent Quality Factor in an Array of Graphene Mechanical Resonators. *Nano Lett.* **2011**, *11*, 1232−1236.

(4) Balandin, A. A. Thermal Properties of Graphene and Nanostructured Carbon Materials. *Nat. Mater.* **2011**, *10*, 569−581.

(5) Mao, L.; Zhang, K.; On Chan, H. S.; Wu, J. Nanostructured Mno2/Graphene Composites for Supercapacitor Electrodes: The Effect of Morphology, Crystallinity and Composition. *J. Mater. Chem.* **2012**, *22*, 1845−1851.

(6) Geim, A. K. Graphene: Status and Prospects. *Science* **2009**, *324*, 1530−1534.

(7) Geim, A. K.; Novoselov, K. S. The Rise of Graphene. *Nat. Mater.* **2007**, *6*, 183−191.

(8) Liao, L.; Lin, Y.-C.; Bao, M.; Cheng, R.; Bai, J.; Liu, Y.; Qu, Y.; Wang, K. L.; Huang, Y.; Duan, X. High-Speed Graphene Transistors with a Self-Aligned Nanowire Gate. *Nature* **2010**, *467*, 305−308.

(9) Levendorf, M. P.; Ruiz-Vargas, C. S.; Garg, S.; Park, J. Transfer-Free Batch Fabrication of Single Layer Graphene Transistors. *Nano Lett.* **2009**, *9*, 4479−4483.

(10) Lin, Y.-M.; Dimitrakopoulos, C.; Jenkins, K. A.; Farmer, D. B.; Chiu, H.-Y.; Grill, A.; Avouris, P. 100-Ghz Transistors from Wafer-Scale Epitaxial Graphene. *Science* **2010**, *327*, 662.

(11) Schedin, F.; Geim, A. K.; Morozov, S. V.; Hill, E. W.; Blake, P.; Katsnelson, M. I.; Novoselov, K. S. Detection of Individual Gas Molecules Adsorbed on Graphene. *Nat. Mater.* **2007**, *6*, 652−655.

(12) Rashad, M.; Pan, F.; Tang, A.; Asif, M. Effect of Graphene Nanoplatelets Addition on Mechanical Properties of Pure Aluminum Using a Semi-Powder Method. *Prog. Nat. Sci.* **2014**, *24*, 101−108.

(13) Novoselov, K. S.; Geim, A. K.; Morozov, S. V.; Jiang, D.; Zhang, Y.; Dubonos, S. V.; Grigorieva, I. V.; Firsov, A. A. Electric Field Effect in Atomically Thin Carbon Films. *Science* **2004**, *306*, 666−669.

(14) Stankovich, S.; Dikin, D. A.; Piner, R. D.; Kohlhaas, K. A.; Kleinhammes, A.; Jia, Y.; Wu, Y.; Nguyen, S. T.; Ruoff, R. S. Synthesis of Graphene-Based Nanosheets Via Chemical Reduction of Exfoliated Graphite Oxide. *Carbon* **2007**, *45*, 1558−1565.

(15) Berger, C.; et al. Ultrathin Epitaxial Graphite: 2d Electron Gas Properties and a Route toward Graphene-Based Nanoelectronics. *J. Phys. Chem. B* **2004**, *108*, 19912−19916.

(16) Mattevi, C.; Kim, H.; Chhowalla, M. A Review of Chemical Vapour Deposition of Graphene on Copper. *J. Mater. Chem.* **2011**, *21*, 3324−3334.

(17) Li, X.; et al. Large-Area Synthesis of High-Quality and Uniform Graphene Films on Copper Foils. *Science* **2009**, *324*, 1312−1314.

(18) Yu, Q.; Lian, J.; Siriponglert, S.; Li, H.; Chen, Y. P.; Pei, S.-S. Graphene Segregated on Ni Surfaces and Transferred to Insulators. *Appl. Phys. Lett.* **2008**, *93*, 113103.

(19) Kim, K. S.; Zhao, Y.; Jang, H.; Lee, S. Y.; Kim, J. M.; Kim, K. S.; Ahn, J.-H.; Kim, P.; Choi, J.-Y.; Hong, B. H. Large-Scale Pattern Growth of Graphene Films for Stretchable Transparent Electrodes. *Nature* **2009**, *457*, 706−710.

(20) Ono, R.; Hosoda, M.; Okuzawa, M.; Tagawa, M.; Oshima, C.; Otani, S. Electronic States of Monolayer Graphene on Pt (755) and Tic (755). *TANSO* **2000**, *2000*, 400−404.

(21) Bae, S.; et al. Roll-to-Roll Production of 30-Inch Graphene Films for Transparent Electrodes. *Nat. Nanotechnol.* **2010**, *5*, 574−578.

(22) Bartelt, N. C.; McCarty, K. F. Graphene Growth on Metal Surfaces. *MRS Bull.* **2012**, *37*, 1158−1165.

(23) Tsen, A. W.; Brown, L.; Levendorf, M. P.; Ghahari, F.; Huang, P. Y.; Havener, R. W.; Ruiz-Vargas, C. S.; Muller, D. A.; Kim, P.; Park, J. Tailoring Electrical Transport across Grain Boundaries in Polycrystalline Graphene. *Science* **2012**, *336*, 1143−1146.

(24) Ajayan, P. M.; Yakobson, B. I. Graphene: Pushing the Boundaries. *Nat. Mater.* **2011**, *10*, 415−417.

(25) Bhaviripudi, S.; Jia, X.; Dresselhaus, M. S.; Kong, J. Role of Kinetic Factors in Chemical Vapor Deposition Synthesis of Uniform Large Area Graphene Using Copper Catalyst. *Nano Lett.* **2010**, *10*, 4128−4133.

(26) Vlassiouk, I.; Regmi, M.; Fulvio, P.; Dai, S.; Datskos, P.; Eres, G.; Smirnov, S. Role of Hydrogen in Chemical Vapor Deposition Growth of Large Single-Crystal Graphene. *ACS Nano* **2011**, *5*, 6069−6076.

(27) Yan, Z.; Lin, J.; Peng, Z.; Sun, Z.; Zhu, Y.; Li, L.; Xiang, C.; Samuel, E. L.; Kittrell, C.; Tour, J. M. Toward the Synthesis of Wafer-Scale Single-Crystal Graphene on Copper Foils. *ACS Nano* **2012**, *6*, 9110−9117.

(28) Wang, H.; Wang, G.; Bao, P.; Yang, S.; Zhu, W.; Xie, X.; Zhang, W.-J. Controllable Synthesis of Submillimeter Single-Crystal Monolayer Graphene Domains on Copper Foils by Suppressing Nucleation. *J. Am. Chem. Soc.* **2012**, *134*, 3627−3630.

(29) Zhang, X.; Wang, L.; Xin, J.; Yakobson, B. I.; Ding, F. Role of Hydrogen in Graphene Chemical Vapor Deposition Growth on a Copper Surface. *J. Am. Chem. Soc.* **2014**, *136*, 3040−3047.

(30) Balooch, M.; Cardillo, M. J.; Miller, D. R.; Stickney, R. E. Molecular Beam Study of the Apparent Activation Barrier Associated with Adsorption and Desorption of Hydrogen on Copper. *Surf. Sci.* **1974**, *46*, 358−392.

(31) Choubak, S.; Biron, M.; Levesque, P. L.; Martel, R.; Desjardins, P. No Graphene Etching in Purified Hydrogen. *J. Phys. Chem. Lett.* **2013**, *4*, 1100−1103.

(32) Hao, Y.; et al. The Role of Surface Oxygen in the Growth of Large Single-Crystal Graphene on Copper. *Science* **2013**, *342*, 720−723.

(33) Lisi, N.; Buonocore, F.; Dikonimos, T.; Leoni, E.; Faggio, G.; Messina, G.; Morandi, V.; Ortolani, L.; Capasso, A. Rapid and Highly Efficient Growth of Graphene on Copper by Chemical Vapor Deposition of Ethanol. *Thin Solid Films* **2014**, *571* (Part 1), 139−144.

(34) Faggio, G.; Capasso, A.; Messina, G.; Santangelo, S.; Dikonimos, T.; Gagliardi, S.; Giorgi, R.; Morandi, V.; Ortolani, L.; Lisi, N. High-Temperature Growth of Graphene Films on Copper Foils by Ethanol Chemical Vapor Deposition. *J. Phys. Chem. C* **2013**, *117*, 21569−21576.

(35) Zhao, P.; Kumamoto, A.; Kim, S.; Chen, X.; Hou, B.; Chiashi, S.; Einarsson, E.; Ikuhara, Y.; Maruyama, S. Self-Limiting Chemical Vapor Deposition Growth of Monolayer Graphene from Ethanol. *J. Phys. Chem. C* **2013**, *117*, 10755−10763.

(36) Feng, J.-M.; Dai, Y.-J. Water-Assisted Growth of Graphene on Carbon Nanotubes by the Chemical Vapor Deposition Method. *Nanoscale* **2013**, *5*, 4422−4426.

(37) Hata, K.; Futaba, D. N.; Mizuno, K.; Namai, T.; Yumura, M.; Iijima, S. Water-Assisted Highly Efficient Synthesis of Impurity-Free Single-Walled Carbon Nanotubes. *Science* **2004**, *306*, 1362−1364.

(38) Yoshihara, N.; Ago, H.; Tsuji, M. Chemistry of Water-Assisted Carbon Nanotube Growth over Fe−Mo/Mgo Catalyst. *J. Phys. Chem. C* **2007**, *111*, 11577−11582.

DOI: 10.1021/jp510106w
J. Phys. Chem. C 2015, 119, 3079−3089

(39) Zhang, X.; Xu, Z.; Hui, L.; Xin, J.; Ding, F. How the Orientation of Graphene Is Determined During Chemical Vapor Deposition Growth. *J. Phys. Chem. Lett.* **2012**, *3*, 2822−2827.
(40) Fan, Y.; Yangqiao, L.; Wei, W.; Wei, C.; Lian, G.; Jing, S. A Facile Method to Observe Graphene Growth on Copper Foil. *Nanotechnology* **2012**, *23*, 475705.
(41) Li, X.; et al. Graphene Films with Large Domain Size by a Two-Step Chemical Vapor Deposition Process. *Nano Lett.* **2010**, *10*, 4328−4334.
(42) Celebi, K.; Cole, M. T.; Teo, K. B. K.; Park, H. G. Observations of Early Stage Graphene Growth on Copper. *Electrochem. Solid-State Lett.* **2012**, *15*, K1−K4.
(43) Srivastava, A.; Galande, C.; Ci, L.; Song, L.; Rai, C.; Jariwala, D.; Kelly, K. F.; Ajayan, P. M. Novel Liquid Precursor-Based Facile Synthesis of Large-Area Continuous, Single, and Few-Layer Graphene Films. *Chem. Mater.* **2010**, *22*, 3457−3461.
(44) Li, Z.; Wu, P.; Wang, C.; Fan, X.; Zhang, W.; Zhai, X.; Zeng, C.; Li, Z.; Yang, J.; Hou, J. Low-Temperature Growth of Graphene by Chemical Vapor Deposition Using Solid and Liquid Carbon Sources. *ACS Nano* **2011**, *5*, 3385−3390.
(45) Zhang, B.; Lee, W. H.; Piner, R.; Kholmanov, I.; Wu, Y.; Li, H.; Ji, H.; Ruoff, R. S. Low-Temperature Chemical Vapor Deposition Growth of Graphene from Toluene on Electropolished Copper Foils. *ACS Nano* **2012**, *6*, 2471−2476.
(46) Li, J.; Kazakov, A.; Dryer, F. L. Experimental and Numerical Studies of Ethanol Decomposition Reactions. *J. Phys. Chem. A* **2004**, *108*, 7671−7680.
(47) Alstrup, I.; Chorkendorff, I.; Ullmann, S. The Interaction of CH_4 at High Temperatures with Clean and Oxygen Precovered Cu(100). *Surf. Sci.* **1992**, *264*, 95−102.
(48) Lawson, A.; Thomson, S. J. 365. Methanol Decomposition on Partially Oxidised Copper Metal. Part I. *J. Chem. Soc. (Resumed)* **1964**, 1861−1880.
(49) Zhang, W.; Wu, P.; Li, Z.; Yang, J. First-Principles Thermodynamics of Graphene Growth on Cu Surfaces. *J. Phys. Chem. C* **2011**, *115*, 17782−17787.
(50) Alstrup, I.; Chorkendorff, I.; Ullmann, S. The Interaction of CH_4 at High Temperatures with Clean and Oxygen Precovered Cu(100). *Surf. Sci.* **1992**, *264*, 95−102.
(51) Galea, N. M.; Knapp, D.; Ziegler, T. Density Functional Theory Studies of Methane Dissociation on Anode Catalysts in Solid-Oxide Fuel Cells: Suggestions for Coke Reduction. *J. Catal.* **2007**, *247*, 20−33.
(52) Gao, L.; Ren, W.; Zhao, J.; Ma, L.-P.; Chen, Z.; Cheng, H.-M. Efficient Growth of High-Quality Graphene Films on Cu Foils by Ambient Pressure Chemical Vapor Deposition. *Appl. Phys. Lett.* **2010**, *97*, -.
(53) Gelb, A.; Cardillo, M. Classical Trajectory Studies of Hydrogen Dissociation on a Cu(100) Surface. *Surf. Sci.* **1976**, *59*, 128−140.
(54) Gelb, A.; Cardillo, M. J. Classical Trajectory Study of the Dissociation of Hydrogen on Copper Single Crystals: II. Cu(100) and Cu(110). *Surf. Sci.* **1977**, *64*, 197−208.

DOI: 10.1021/jp510106w
J. Phys. Chem. C 2015, 119, 3079−3089